Lumen boundaries extracted from coronary computed tomography angiography on computed fractional flow reserve (FFR$_{CT}$): validation with optical coherence tomography

Kenzo Uzu[1], MD; Hiromasa Otake[1]*, MD; Gilwoo Choi[1], PhD; Takayoshi Toba[1], MD;
Hyun Jin Kim[1], PhD; Arjun Roy[2], BS; Michiel Schaap[2], PhD; Leo Grady[2], PhD;
Masahito Kawata[3], MD; Toshiro Shinke[1], MD; Charles A. Taylor[2,4], PhD; Ken-ichi Hirata[1], MD

1. Division of Cardiovascular Medicine, Department of Internal Medicine, Kobe University Graduate School of Medicine, Hyogo, Japan; 2. HeartFlow, Inc., Redwood City, CA, USA; 3. Department of Cardiology, Akashi Medical Center, Hyogo, Japan; 4. Department of Bioengineering, Stanford University, Stanford, CA, USA

This paper also includes supplementary data published online at: http://www.pcronline.com/eurointervention/148th_issue/274

KEYWORDS

- fractional flow reserve
- MSCT
- non-invasive imaging
- optical coherence tomography

Abstract

Aims: The aim of this study was to evaluate the accuracy of minimum lumen area (MLA) by coronary computed tomography angiography (cCTA) and its impact on fractional flow reserve (FFR$_{CT}$).

Methods and results: Fifty-seven patients (118 lesions, 72 vessels) who underwent cCTA and optical coherence tomography (OCT) were enrolled. OCT and cCTA were co-registered and MLAs were measured with both modalities. FFR$_{OCT}$ was calculated using OCT-updated models with cCTA-based lumen geometry replaced by OCT-derived geometry. Lesions were grouped by Agatston score (AS) and minimum lumen diameter (MLD) using the OCT catheter and guidewire size (1.0 mm) as a threshold. For all lesions, the average absolute difference between cCTA and OCT MLA was 0.621±0.571 mm^2. Pearson correlation coefficients between cCTA and OCT MLAs in lesions with low-intermediate and high AS were 0.873 and 0.787, respectively (both p<0.0001). Irrespective of AS score, excellent correlations were observed for MLA (r=0.839, p<0.0001) and FFR comparisons (r=0.918, p<0.0001) in lesions with MLD ≥1.0 mm but not for lesions with MLD <1.0 mm.

Conclusions: The spatial resolution of cCTA or calcification does not practically limit the accuracy of lumen boundary identification by cCTA or FFR$_{CT}$ calculations for MLD ≥1.0 mm. The accuracy of cCTA MLA could not be adequately assessed for lesions with MLD <1.0 mm.

Corresponding author: Department of Cardiology, Kobe University Graduate School of Medicine, 7-5-1 Kusunoki-cho, Chuo-ku, Kobe, Hyogo, 650-0017, Japan. E-mail: hotake@med.kobe-u.ac.jp

Abbreviations

AS   Agatston score

cCTA   coronary computed tomography angiography

FFR   fractional flow reserve

FFR_{CT}   fractional flow reserve derived from coronary computed tomography angiography

FFR_{OCT}   re-computed FFR_{CT} value in a model updated using optical coherence tomography data

MLA   minimum lumen area

MLD   minimum lumen diameter

OCT   optical coherence tomography

Introduction

Recently, application of computational fluid dynamics technology to coronary computed tomographic angiography (cCTA) images has enabled computation of coronary artery blood flow and pressure, and calculation of fractional flow reserve (FFR), without an invasive procedure[1]. This method, fractional flow reserve derived from coronary computed tomography angiography (FFR_{CT}), has demonstrated a high diagnostic accuracy for detection of ischaemia using invasive FFR as the reference standard[2,3], substantiating its potential as a reliable gatekeeper to invasive coronary angiography.

Despite clinical data, it has been hypothesised that the limited spatial resolution of cCTA may impose significant limitations on the accuracy of FFR_{CT}[4]. Additionally, coronary calcification might hamper accurate estimation of FFR by cCTA, given potential difficulties in lumen border detection due to calcium blooming. Therefore, in this study, we prospectively evaluated the accuracy of the semi-automated lumen boundary extracted from cCTA (HeartFlow FFR_{CT} software version 1.8; HeartFlow, Redwood City, CA, USA) and its impact on FFR_{CT} along the vessel using optical coherence tomography (OCT) data as the reference standard.

Methods

STUDY POPULATION

At two centres in Japan (Kobe University Hospital and Akashi Medical Center), 100 patients with available preprocedural cCTA and OCT data within six months between examinations were enrolled **(Supplementary Appendix 1)**. Patients who underwent clinically indicated coronary angiography and OCT with preprocedural cCTA were eligible for inclusion. Among such patients, lesions with a percentage diameter stenosis between 25% and 75% by angiography were considered for quantitative cCTA and OCT analysis. Each vessel was divided into several lesions based on the side branches (>1.5 mm) to compare lumen areas. We measured the cross-sectional area from CT and OCT lesions, and identified the minimum lumen area (MLA) over the lesion for comparison. To ensure that the vessel diameter was larger than the catheter size, we also measured the linear minimum lumen diameter (MLD) in OCT using a proprietary OCT workstation (St. Jude Medical, St. Paul, MN, USA). MLD was directly computed from the points on the cross-sectional contour instead of

being derived from the cross-sectional area that requires a circular cross-sectional assumption. The linear MLD was used to divide the MLA measurement data for a subgroup analysis in OCT and CT MLA comparison. The study endpoints are described in **Supplementary Appendix 2**.

The study protocol was approved by the institutional review boards of each participating centre, and all patients gave written informed consent.

CORONARY CT ANGIOGRAPHY IMAGE ACQUISITION AND ANALYSIS

cCTA images were obtained in accordance with the Society of Cardiovascular Computed Tomography (SCCT) guidelines on cCTA[5]. Detailed CT acquisition protocol, parameters and image quality analysis are described in **Supplementary Appendix 3-Supplementary Appendix 5**. To assess the impact of image quality on the MLA comparison, the signal-to-noise ratio (SNR), contrast-to-noise ratio (CNR), and five-point Likert scale score were calculated, as previously described[6].

Quantitative cCTA analysis was performed by HeartFlow, Inc., in a blinded fashion as previously described[1,7]. The coronary calcium scores for each coronary artery were independently assessed by a CT core laboratory in Kobe University according to the Agatston method[8]. Agatston score (AS) was evaluated in each vessel.

OCT EXAMINATION AND ANALYSIS

OCT (C7 Dragonfly™; St. Jude Medical, St. Paul, MN, USA) was performed as previously reported[9]. Off-line OCT analysis was performed to measure cross-sectional area and MLD using a dedicated workstation in the Kobe University OCT core laboratory blinded to the cCTA results. Lumen contours were automatically delineated every 0.2 mm, followed by a manual modification if necessary. Since the size of guidewire and catheter (0.014-inch and 0.9 mm in diameter, respectively[9]) limits MLD quantification in OCT **(Supplementary Figure 1)**, we divided the vessels (lesions) according to MLD ≥1.0 mm (above the catheter size) and MLD <1.0 mm (below the catheter size) by OCT to isolate potential errors in OCT measurements.

CO-REGISTRATION OF CT WITH OCT DATA AND COMPARISON OF MLA

After unblinding the cCTA and OCT case numbers, the OCT image was co-registered to cCTA data. Briefly, a 3D-OCT model was first constructed by stacking OCT lumen contours along the vessel length. Next, cCTA-derived lumen geometry was straightened along the centreline using a cylindrical coordinate transformation[10], and the 3D-OCT model was aligned to the straightened cCTA lumen geometry **(Figure 1A)**. Then, the 3D-OCT model was stretched and twisted to match the straightened cCTA-derived model based on branch ostia **(Figure 1B)**. The co-registered OCT model was bent to the original curved-cCTA space **(Figure 1C)**. Finally, MLAs from OCT and cCTA were detected and compared **(Figure 1D)**.
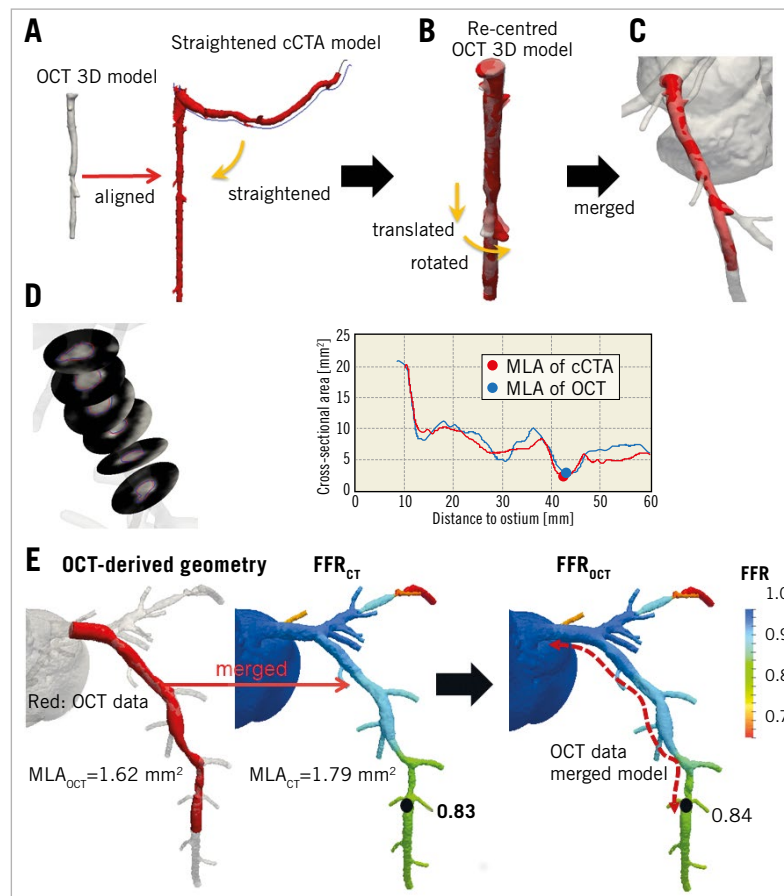
Figure 1. *Co-registration of cCTA and OCT images. A) OCT 3D model constructed by stacking 2D slices and straightened cCTA model. B) OCT 3D model re-centred to centroid of each cross-section and illustration of translation and rotation of model. C) OCT 3D model co-registered to cCTA model. D) Cross-sectional contour images and area of co-registered OCT data with cCTA data. E) FFR$_{CT}$ evaluation in OCT-merged model.*

COMPARISON OF FFR$_{CT}$ WITH COMPUTED FFR DERIVED FROM OCT-MERGED CORONARY MODEL

To assess the impact of lumen boundary accuracy extracted from cCTA on FFR$_{CT}$, we compared the original FFR$_{CT}$ with re-computed FFR$_{CT}$ values in a model updated using OCT data, i.e., FFR$_{OCT}$. Specifically, the OCT-derived lumen model was used to replace the cCTA-derived coronary model on corresponding vessel segments using the co-registration method described above **(Figure 1E)**. To evaluate the true effect of segments updated by OCT on FFR$_{CT}$, all the other arteries and side branches were unchanged. Consequently, all boundary conditions remained the same in the evaluation of FFR$_{OCT}$ as in the original FFR$_{CT}$ computation[1,7]. The comparison of FFR$_{CT}$ with FFR$_{OCT}$ was performed on a per-vessel basis at the location immediately distal to the OCT segment; a computed FFR ≤0.8 was considered diagnostic of lesion-specific ischaemia.

STATISTICAL ANALYSIS

The sample size calculation is described in **Supplementary Appendix 6**. Normally distributed continuous variables were expressed as mean±SD and were compared with two-tailed unpaired t-tests, whereas non-normally distributed continuous variables were expressed as median (interquartile ranges) and compared using the Mann-Whitney U test. Correlation was assessed by linear correlation; mean differences and limits of agreement were assessed by Bland-Altman analysis. The agreement between the two methods was also assessed by the Passing-Bablok method. The Fisher z-transformation statistic was applied for comparing two correlations and the F-test was used to compare variation. A p-value of 0.05 or less was considered statistically significant. All statistical analyses were performed using a commercial software package (SPSS, Version 24.0; IBM Corp., Armonk, NY, USA, and XLSTAT version 2017; Addinsoft, New York, NY, USA).

Results

BASELINE PATIENT AND LESION CHARACTERISTICS

From 100 patients, 137 vessels were considered for inclusion in the present study. After excluding 65 vessels, 72 vessels (118 lesions) in 57 patients were included for MLA comparisons. Also,

eight vessels were excluded from FFR computation due to the lack of side branches; therefore, we assessed the difference between cCTA and OCT-based FFR in 64 vessels representing 52 patients **(Figure 2, Supplementary Appendix 7)**. Baseline patient and lesion characteristics are summarised in **Table 1**.

Table 1. Baseline patient and lesion characteristics.

Patient characteristics (n=57)		
Age, years		69.4±10.4
Female, n (%)		17 (29.8)
BMI, kg/m^2		25.4±5.2
cCTA acquisition heart rate, beats/min		60.7±6.6
Interval between cCTA and OCT, days		47.0±48.8
Hypertension, n (%)		42 (73.7)
Dyslipidaemia, n (%)		42 (73.7)
Diabetes mellitus, n (%)		24 (42.1)
Current smoking, n (%)		7 (12.3)
Familial history of coronary artery disease, n (%)		6 (10.5)
Lesion characteristics (n=72)		
Studied vessel	Left anterior descending, n (%)	34 (47.2)
	Left circumflex, n (%)	15 (20.8)
	Right coronary artery, n (%)	23 (31.9)
	Per-vessel Agatston score	192.9±226.9
	Low (0-31.2), n (%)	24 (33.3)
	Intermediate (31.2-192.2), n (%)	24 (33.3)
	High (192.2-966.4), n (%)	24 (33.3)

Values are median±SD or n (%). BMI: body mass index; cCTA: coronary computed tomography angiography; OCT: optical coherence tomography

COMPARISONS OF MLA AND COMPUTED FFR BETWEEN cCTA AND OCT

Overall, there was no significant difference in the average cCTA and OCT MLAs **(Table 2)**. The average absolute difference in MLA measurements between cCTA and OCT was 0.621±0.571 mm^2, with an excellent correlation between the two imaging modalities (r=0.851, p<0.0001) **(Figure 3A)**. Bland-Altman plots of cCTA MLA in relation to OCT MLA showed a mean bias of –0.018±1.652 mm^2 with 95% limits of agreement of –1.671 to 1.633 mm^2 **(Figure 3B)**.

For computed FFR, FFR_{CT} tended to be lower than FFR_{OCT} **(Table 2)**. There was a significant positive correlation between FFR_{CT} and FFR_{OCT} (r=0.778, p<0.0001) **(Figure 3C)**. Bland-Altman plots of FFR_{CT} in relation to FFR_{OCT} showed a mean bias of –0.047±0.185 with 95% limits of agreement of –0.231 to 0.138 **(Figure 3D)**.

No difference was observed in the MLA, MLD, and FFR values between cCTA and OCT in 64-slice, 128-slice, and 320-slice cCTA **(Supplementary Table 1)**. Additionally, image quality measured on the basis of the SNR, CNR, and five-point Likert scale score did not impact on the accuracy of cCTA measurements compared with OCT **(Supplementary Table 2-Supplementary Table 4)**. Significant positive correlations were observed between cCTA and OCT MLAs in lesions with low and intermediate-high image qualities **(Supplementary Figure 2)**.

COMPARISONS OF MLA AND COMPUTED FFR BETWEEN cCTA AND OCT IN LESIONS WITH MLD ≥1.0 mm AND <1.0 mm

When all lesions were divided according to OCT MLD measurements, there was no significant difference in the cCTA and OCT MLAs in lesions with both MLD ≥1.0 mm and MLD <1.0 mm
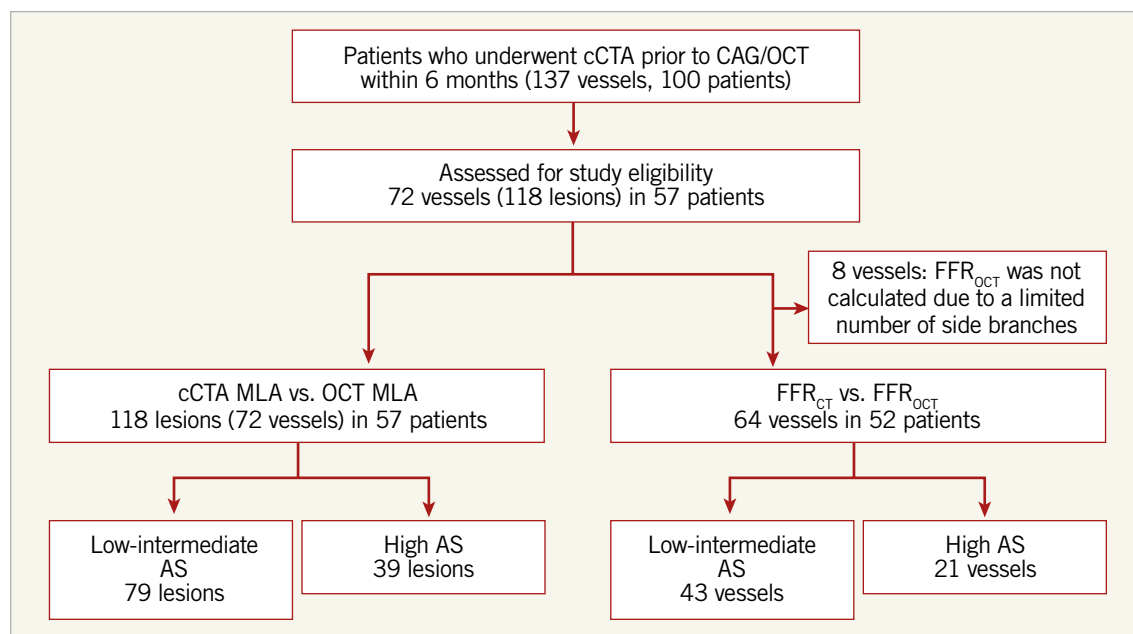

Figure 2. *Study population flow chart. AS: Agatston score; CAG: coronary angiography; cCTA: coronary computed tomography angiography; FFR: fractional flow reserve; MLA: minimum lumen area; OCT: optical coherence tomography*

Table 2. Comparisons of cCTA and OCT measurements.

	All (118 lesions, 72 vessels)			MLD ≥1.0 mm (93 lesions, 60 vessels)			MLD <1.0 mm (25 lesions, 23 vessels)		
	cCTA	OCT	*p*-value	cCTA	OCT	*p*-value	cCTA	OCT	*p*-value
MLA (mm²)	2.37±1.59	2.39±1.51	0.926	2.72±1.57	2.80±1.45	0.732	1.05±0.79	0.86±0.14	0.238
MLD (mm)	0.82±0.28	0.83±0.26	0.783	1.79±0.50	1.83±0.46	0.606	1.09±0.41	1.04±0.09	0.608
FFR value	0.743±0.151	0.790±0.113	0.051	0.792±0.108	0.823±0.098	0.166	0.644±0.179	0.722±0.116	0.101

Values are median±SD. cCTA: coronary computed tomography angiography; FFR: fractional flow reserve; MLA: minimum lumen area; MLD: minimum lumen diameter; OCT: optical coherence tomography
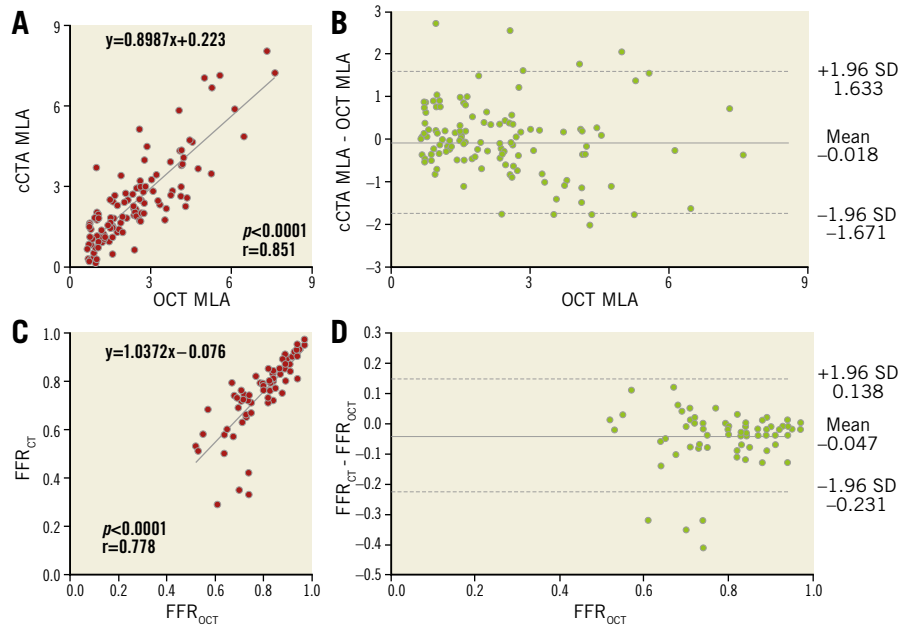
Figure 3. *cCTA vs. OCT measurement in the overall population. A) Correlation between MLA from cCTA and OCT. B) Bland-Altman plots of cCTA MLA versus OCT MLA. C) Correlation between FFR from cCTA and OCT. D) Bland-Altman plots of FFR$_{CT}$ vs. FFR$_{OCT}$*

(Table 2). There was a significant positive correlation between the cCTA and OCT MLAs in lesions with MLD ≥1.0 mm (r=0.839, p<0.0001) **(Figure 4A.a)**, whilst the positive correlation was weaker and biased downward in lesions with MLD <1.0 mm (r=0.282, p=0.172) **(Figure 4B.a)**, which was statistically different (p<0.0001). Bland-Altman plots of the cCTA MLA in relation to the OCT MLA showed a mean bias of –0.076±1.683 for lesions with MLD ≥1.0 mm and of 0.193±1.458 for those with MLD <1.0 mm **(Figure 4A.b, Figure 4B.b)**. There was no significant difference in variation between the two groups (F=2.006, p=0.159). For computed FFR, there was no significant difference in the average value of FFR$_{CT}$ and FFR$_{OCT}$ between vessels in both groups with MLD ≥1.0 mm and MLD <1.0 mm **(Table 2)**. There were significant positive correlations between FFR$_{CT}$ and FFR$_{OCT}$ in vessels with MLD ≥1.0 mm (r=0.918, p<0.0001) **(Figure 4A.c)** and MLD <1.0 mm (r=0.543, p=0.011) **(Figure 4B.c)**. In the Bland-Altman plots, 95% limits of agreement for vessels with MLD <1.0 mm tended to be wider than for vessels with MLD ≥1.0 mm (–0.368 to 0.211 vs. –0.114 to 0.052; F=3.702, p=0.059) **(Figure 4B.d, Figure 4A.d)**. The Passing-Bablok method showed the same trend **(Supplementary Table 5)**.

COMPARISONS OF MLA AND FFR BETWEEN cCTA AND OCT ACCORDING TO THE SEVERITY OF CALCIFICATION

AS distribution is shown in **Supplementary Figure 3**. There was no significant difference between the average cCTA and OCT MLAs in lesions with both low-intermediate and high AS **(Table 3)**. The average absolute difference of MLA between cCTA and OCT measurements was comparable in lesions with both low-intermediate and high AS (0.609±0.587 mm² vs. 0.681±0.570 mm²; p=0.422, respectively). There was a significant positive correlation between cCTA and OCT MLAs in lesions with low-intermediate AS (r=0.873, p<0.0001) **(Figure 5A.a)** and high AS (r=0.787, p<0.0001) **(Figure 5B.a)**. There was no significant difference in the strength of correlation between the two groups (p=0.163). Bland-Altman plots of the cCTA MLA in relation to the OCT MLA showed a mean bias of –0.047±1.604 for lesions with low-intermediate AS and of 0.039±1.740 for lesions with high AS **(Figure 5A.b, Figure 5B.b)**. No significant difference was observed in variation between the two groups (F=0.268, p=0.606).

There was no significant difference between the mean FFR$_{CT}$ and FFR$_{OCT}$ values in vessels with low-intermediate and high AS

Table 3. Comparisons of cCTA and OCT measurements in lesions with low-intermediate and high AS.

	Low-intermediate AS (79 lesions, 48 vessels)			High AS (39 lesions, 24 vessels)		
	cCTA	OCT	*p*-value	cCTA	OCT	*p*-value
MLA (mm²)	2.48±1.67	2.53±1.59	0.855	2.14±1.42	2.11±1.31	0.901
MLD (mm)	0.84±0.29	0.86±0.27	0.716	0.79±0.25	0.78±0.24	0.945
FFR value	0.737±0.160	0.793±0.115	0.070	0.755±0.134	0.784±0.112	0.140
AS: per-vessel Agatston score; cCTA: coronary computed tomography angiography; FFR: fractional flow reserve; MLA: minimum lumen area; MLD: minimum lumen diameter; OCT: optical coherence tomography						

(Table 3). There were strong correlations between FFR_{CT} and FFR_{OCT} in vessels with low-intermediate (r=0.791, p<0.0001) **(Figure 5A.c)** and high AS (r=0.766, p<0.0001) **(Figure 5B.c)**, and no significant difference in the strength of correlation between the two groups (p=0.823). Bland-Altman plots of FFR_{CT} in relation to FFR_{OCT} showed mean biases of −0.055±0.191 and 0.058±0.134
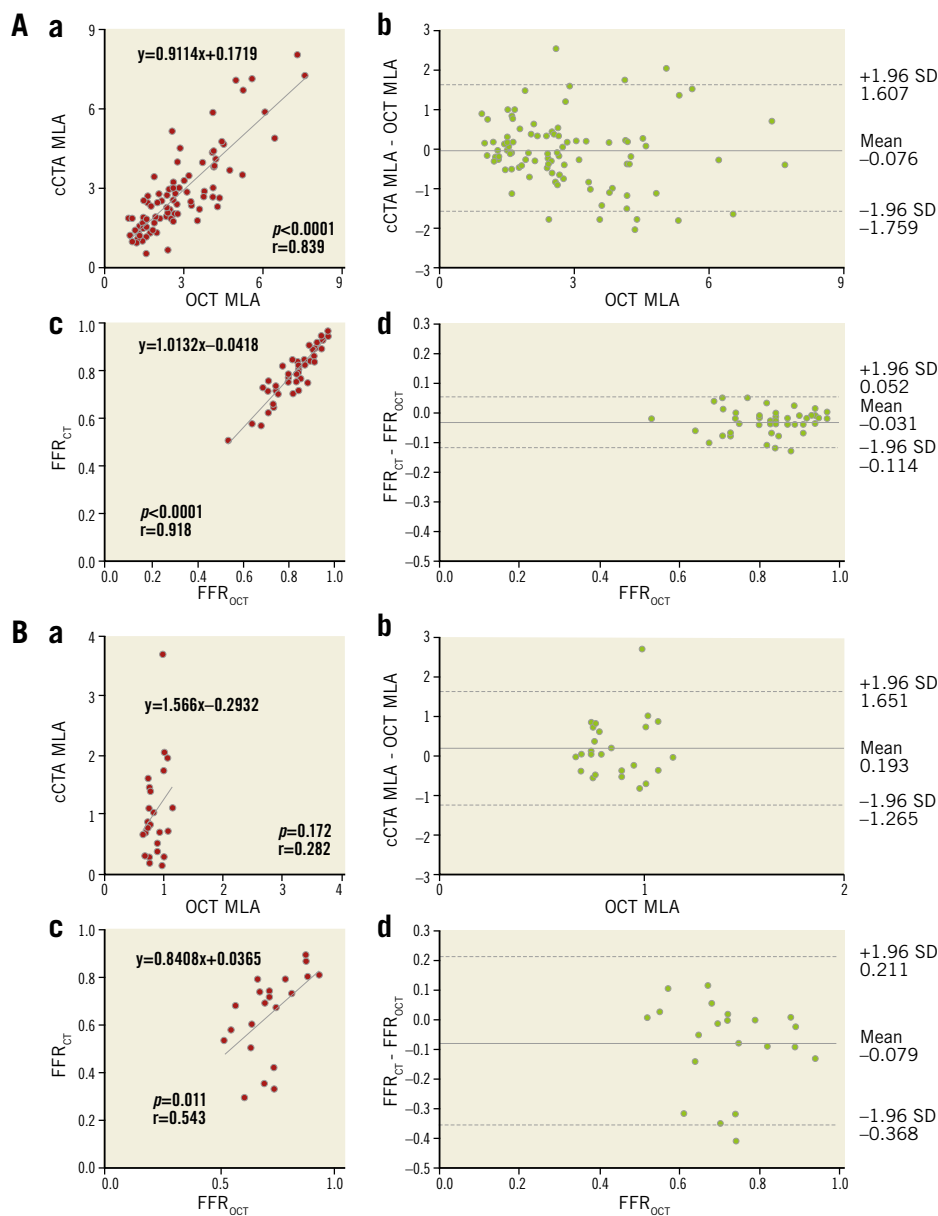

Figure 4. *cCTA vs. OCT measurement. A) Lesions with MLD above the catheter size (MLD ≥1.0 mm) and B) MLD below the catheter size (MLD <1.0 mm). a) Correlation between MLA from cCTA and OCT; b) Bland-Altman plots of cCTA MLA vs. OCT MLA; c) correlation between FFR from cCTA and OCT; d) Bland-Altman plots of FFR_{CT} vs. FFR_{OCT}*
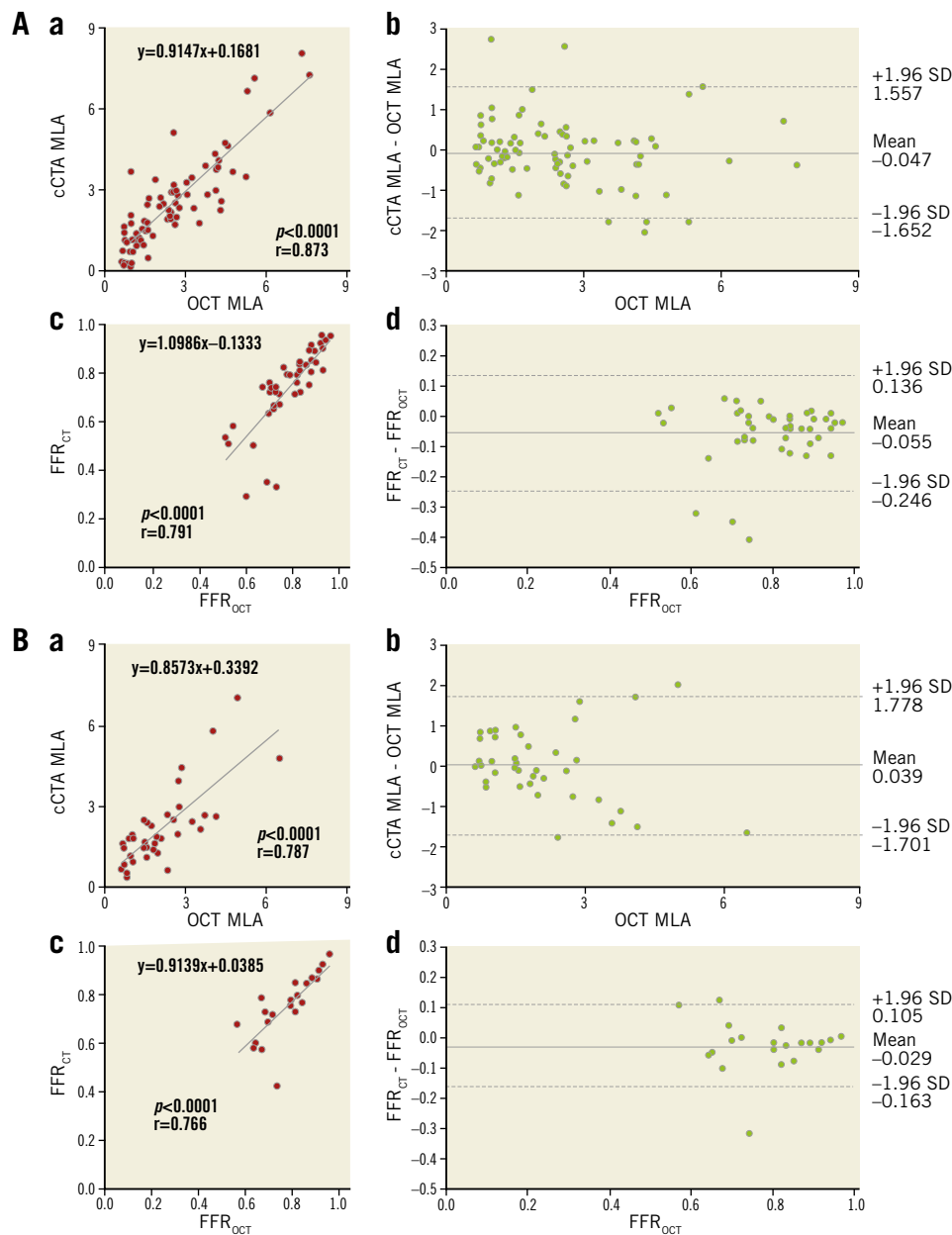
Figure 5. *cCTA vs. OCT measurement. A) Lesions with low-intermediate AS and B) lesions with severe AS. a) Correlation between MLA from cCTA and OCT; b) Bland-Altman plots of cCTA MLA vs. OCT MLA; c) correlation between FFR from cCTA and OCT; d) Bland-Altman plots of FFR$_{CT}$ versus FFR$_{OCT}$*

for vessels with low-intermediate and high AS, respectively **(Figure 5A.d, Figure 5B.d)**. There was no significant difference in variation between the two groups (F=1.061, p=0.307).

CONCORDANCE RATE OF DETECTING ISCHAEMIA BETWEEN FFR$_{CT}$ AND FFR$_{OCT}$

The overall concordance rate between FFR$_{CT}$ and FFR$_{OCT}$ was 82.8% **(Supplementary Figure 4)**. Representative concordant and discordant cases are shown in **Supplementary Figure 5-Supplementary Figure 7**.

Discussion

IMPACT OF IMAGE QUALITY ON GEOMETRIC ACCURACY

The pressure loss along the coronary artery is affected by the coronary artery anatomy and blood flow. Among various geometric features of coronary lesions, MLA and lesion length are two of the most critical parameters affecting coronary flow and pressure. Thus, accurate computation of FFR by cCTA necessitates an accurate representation of coronary lumen geometry. A recent substudy of the DeFACTO trial demonstrated the importance of administering beta-blocker and adequate nitrate dosage recommended

by SCCT guidelines to ensure high image quality[5]. Specifically, cases with appropriate imaging protocol exhibited improved specificity of FFR_{CT} (66.0% vs. 51.0%; p=0.03) and significantly lower bias (−0.048 vs. −0.084; p=0.008)[11]. Additionally, cases without misaligned artefacts demonstrated improved sensitivity (86.0% vs. 43.0%; p=0.001) and overall diagnostic accuracy (71.0% vs. 56.0%; p=0.03). These data suggest the importance of image quality, which can potentially impact on the creation of accurate patient-specific geometric models, leading to accurate FFR computation by cCTA.

In the present study, a high agreement between cCTA- and OCT-based MLA measurements was observed over a broad spectrum of cCTA image qualities measured by SNR (6.7-41.3), CNR (12.8-73.7), and five-point Likert scale (2-5). Johnson et al stated that limits in the spatial resolution of cCTA could introduce large errors in stenosis diameter and even greater errors in stenosis resistance, pressure drop, and calculated FFR_{CT} based on a simple idealised coronary resistance model approximated from the MLD of the vessel[4]. In the present study, however, the average absolute difference of effective MLD between cCTA and OCT measurements was 0.239±0.200 mm, which is much smaller than the typical image resolution of cCTA (e.g., 0.6 mm). Furthermore, instead of amplified errors, a strong correlation (r=0.778) was observed between FFR_{CT} and FFR_{OCT} with only a small difference between the average FFR_{CT} and FFR_{OCT} in the overall population. In lesions with MLD above the catheter size (MLD ≥1.0 mm), an excellent correlation (r=0.918) was observed with no difference in the average values.

Possible explanations for the smaller MLA errors observed in the present study other than the typical cCTA image resolution are as follows. First, the impact of image resolution on MLA estimation can be reduced because cCTA produces greyscale – not binary (black and white) – images. Second, in greyscale images, it would be extremely unlikely to underestimate or overestimate the lumen size with one pixel consistently over the entire circumference of the cross-sectional lumen boundary. Third, image processing algorithms can utilise prior information on the shape of the vessel in all three-dimensional directions, which can be augmented with image intensity information in the lumen extraction process. Therefore, despite the limited resolution of inherent cCTA data, sub-pixel (or sub-voxel) resolution can be attained with computer-automated image segmentation methods.

POTENTIAL ISSUES WITH COMPARING cCTA-DERIVED MLA AND FFR_{CT} WITH OCT MEASUREMENTS IN TIGHT LESIONS

In lesions larger than the catheter size (MLD ≥1.0 mm), a strong positive correlation was observed between cCTA and OCT MLAs. However, in lesions smaller than the catheter size (MLD <1.0 mm), a weak correlation was observed. One possible explanation could be the inaccurate lumen quantification by OCT in lesions with MLD <1.0 mm. The diameter of the OCT imaging catheter was approximately 0.9 mm[9]; therefore, when evaluated by OCT, lumen dimensions can become enlarged or reduced, especially in tight lesions. Another possibility is that lumen measurement by cCTA

is inaccurate in lesions with severe stenosis. *In vitro* validation of cCTA showed that cCTA underestimated the lumen size in lesions with MLD <1.0 mm[12]. Although both studies used the same cut-off value of 1.0 mm for subgroup analyses, the motivation of using 1.0 mm MLD as the cut-off value to divide data was different. We chose 1.0 mm based on the invasive catheter size to collect reliable OCT MLA measurements **(Supplementary Figure 1)**. Moreover, there exist fundamental differences in methods between the two studies, including imaging objects (phantom vs. patient), physiologic conditions (steady vs. pulsatile), plaques (none vs. present), imaging artefacts (none vs. present), and segmentation algorithm. Although it is possible that the spatial resolution of cCTA affected the underestimation of the lumen size in lesions with MLD <1.0 mm, we think that the lumen accuracy for lesions with MLD <1.0 mm is not evaluable using OCT because of the size of the invasive catheter. However, the concordance of FFR_{CT} with FFR_{OCT} was not degraded in lesions with MLD <1.0 mm (overall: 82.8%, lesions with MLD <1.0 mm: 90.5%). Among lesions with MLD <1.0 mm, only one case showed a negative FFR_{CT} but positive FFR_{OCT} result. Even in this case, the discordant diagnosis appeared to be due to the error in OCT measurements caused by the accordion phenomenon **(Supplementary Figure 5)**. Although the accuracy of cCTA MLA for lesions with MLD <1.0 mm could not be evaluated in the present study, these results suggest that FFR_{CT} may provide high diagnostic performance even in vessels with MLD <1.0 mm since the lesion is extremely tight.

POTENTIAL IMPACT OF CORONARY ARTERY CALCIFICATION ON FFR_{CT}

Several studies have shown that coronary calcification is associated with lower cCTA specificity[13,14]. However, Nørgaard et al showed that FFR_{CT} provides superior diagnostic performance over cCTA alone, even in patients with a high AS (per vessel AS range: 121 to 1,703)[15]. In addition, even at the site of metallic markers of a bioresorbable scaffold, Collet et al reported the adequate accuracy of cCTA to assess the luminal dimension by including the centre of the marker in the luminal area[16]. In the present study, even in the highest AS tertile, there was an excellent correlation between FFR simulation by cCTA and OCT, especially in vessels with MLD ≥1.0 mm **(Supplementary Table 6, Supplementary Table 7, Supplementary Figure 8)**. Vessels in the highest AS tertile accounted for only 27.3% of those with a discordant diagnosis. This result suggests that the severity of calcification was not the critical factor affecting the diagnostic accuracy of FFR_{CT}. In vessels with MLD ≥1.0 mm, the correlation coefficient of FFR value between cCTA and OCT was higher than that of MLA in vessels with a high AS **(Supplementary Figure 8)**. This result suggests that FFR_{CT} might be less influenced by coronary calcification in lumen quantification by cCTA. Moreover, the correlation between FFR_{CT} and FFR_{OCT} was higher than that of the MLAs. This phenomenon can be explained by the fact that pressure drop across lesions is determined by total resistance of the lesion integrated over the entire segment of the vessel, rather than a single cross-section.

Study limitations

Several limitations should be noted. First, this study was a non-randomised and retrospective study with a relatively limited sample size. Second, nitroglycerine protocols were not consistent for image acquisitions during cCTA, ICA, and OCT. The difference in nitroglycerine protocol could affect the dimensions of the coronary lumen and potentially influence the comparison results. Third, invasive FFR was not performed. Instead, FFR$_{OCT}$ was used to evaluate the direct impact of geometric accuracy on the computation of FFR resulting from the difference in cCTA and OCT models including resolution and artefacts. Finally, MLAs by OCT and cCTA can originate from different sites. The approach we chose, however, was not based on the exact slice-by-slice comparison. Instead, we defined the lesion of interest using side branches as landmarks to co-register lesions and compared detected minimum areas for the segment. The rationale behind this approach is based on the fact that pressure drop over the lesion is unlikely to be affected by the misaligned MLA locations with a couple of millimetres, but rather the critical parameter is the discrepancy of MLA over the same segment.

Conclusions

The spatial resolution of cCTA does not practically limit the accuracy of lumen boundary identification or affect FFR$_{CT}$. Small lumen diameters, such as those less than 1.0 mm, result in greater discordance between cCTA and OCT MLA values. However, this discordance may be due to the limitation of using the invasive OCT catheter and, nonetheless, has a limited impact on FFR$_{CT}$ diagnostic accuracy. In addition, lumen quantification by cCTA showed high accuracy as compared to OCT data over a wide range of coronary calcification scores. Finally, if the image quality is adequate to calculate FFR$_{CT}$, the image quality does not significantly influence the accuracy of the lumen measurements.

Impact on daily practice

cCTA lumen detection is reliable for FFR$_{CT}$ computations even in severely calcified lesions provided the image quality is acceptable.

Conflict of interest statement

H. Otake and T. Shinke serve as consultants to Abbott Vascular. H. Otake has received honoraria from HeartFlow, Inc. G. Choi, H.J. Kim, M. Schaap, L. Grady, C. Taylor, and A. Roy are employees and/or shareholders of HeartFlow, Inc. The other authors have no conflicts of interest to declare.

References

1. Taylor CA, Fonte TA, Min JK. Computational fluid dynamics applied to cardiac computed tomography for noninvasive quantification of fractional flow reserve: scientific basis. *J Am Coll Cardiol.* 2013;61:2233-41.

2. Norgaard BL, Leipsic J, Gaur S, Seneviratne S, Ko BS, Ito H, Jensen JM, Mauri L, De Bruyne B, Bezerra H, Osawa K, Marwan M, Naber C, Erglis A, Park SJ, Christiansen EH, Kaltoft A, Lassen JF, Botker HE, Achenbach S; NXT Trial Study Group. Diagnostic performance of noninvasive fractional flow reserve derived from coronary computed tomography angiography in suspected coronary artery disease: the NXT trial (Analysis of Coronary Blood Flow Using CT Angiography: Next Steps). *J Am Coll Cardiol.* 2014;63:1145-55.

3. Koo BK, Erglis A, Doh JH, Daniels DV, Jegere S, Kim HS, Dunning A, DeFrance T, Lansky A, Leipsic J, Min JK. Diagnosis of ischemia-causing coronary stenoses by noninvasive fractional flow reserve computed from coronary computed tomographic angiograms. Results from the prospective multicenter DISCOVER-FLOW (Diagnosis of Ischemia-Causing Stenoses Obtained Via Noninvasive Fractional Flow Reserve) study. *J Am Coll Cardiol.* 2011;58:1989-97.

4. Johnson NP, Kirkeeide RL, Gould KL. Coronary anatomy to predict physiology: fundamental limits. *Circ Cardiovasc Imaging.* 2013;6:817-32.

5. Abbara S, Arbab-Zadeh A, Callister TQ, Desai MY, Mamuya W, Thomson L, Weigold WG. SCCT guidelines for performance of coronary computed tomographic angiography: a report of the Society of Cardiovascular Computed Tomography Guidelines Committee. *J Cardiovasc Comput Tomogr.* 2009;3:190-204.

6. Mangold S, Wichmann JL, Schoepf UJ, Caruso D, Tesche C, Steinberg DH, Varga-Szemes A, Stubenrauch AC, Bayer RR 2nd, Biancalana M, Nikolaou K, De Cecco CN. Diagnostic accuracy of coronary CT angiography using 3rd-generation dual-source CT and automated tube voltage selection: clinical application in a non-obese and obese patient population. *Eur Radiol.* 2017;27:2298-308.

7. Min JK, Taylor CA, Achenbach S, Koo BK, Leipsic J, Norgaard BL, Pijls NJ, De Bruyne B. Noninvasive Fractional Flow Reserve Derived From Coronary CT Angiography: Clinical Data and Scientific Principles. *JACC Cardiovasc Imaging.* 2015;8: 1209-22.

8. Agatston AS, Janowitz WR, Hildner FJ, Zusmer NR, Viamonte M Jr, Detrano R. Quantification of coronary artery calcium using ultrafast computed tomography. *J Am Coll Cardiol.* 1990;15:827-32.

9. Gonzalo N, Tearney GJ, Serruys PW, van Soest G, Okamura T, Garcia-Garcia HM, van Geuns RJ, van der Ent M, Ligthart J, Bouma BE, Regar E. Second-generation optical coherence tomography in clinical practice. High-speed data acquisition is highly reproducible in patients undergoing percutaneous coronary intervention. [Article in English, Spanish]. *Rev Esp Cardiol.* 2010;63:893-903.

10. Choi G, Xiong G, Cheng CP, Taylor CA. Methods for characterizing human coronary artery deformation from cardiac-gated computed tomography data. *IEEE Trans Biomed Eng.* 2014;61: 2582-92.

11. Leipsic J, Yang TH, Thompson A, Koo BK, Mancini GB, Taylor C, Budoff MJ, Park HB, Berman DS, Min JK. CT angiography (CTA) and diagnostic performance of noninvasive fractional flow reserve: results from the Determination of Fractional Flow Reserve by Anatomic CTA (DeFACTO) study. *AJR Am J Roentgenol.* 2014;202:989-94.

12. Collet C, Onuma Y, Grundeken MJ, Miyazaki Y, Bittercourt M, Kitslaar P, Motoyama S, Ozaki Y, Asano T, Wentzel JJ, Streekstra GJ, Serruys PW, de Winter RJ, Planken N. In vitro validation of coronary CT angiography for the evaluation of complex lesions. *EuroIntervention.* 2018;13:e1823-30.

13. Yan RT, Miller JM, Rochitte CE, Dewey M, Niinuma H, Clouse ME, Vavere AL, Brinker J, Lima JA, Arbab-Zadeh A. Predictors of inaccurate coronary arterial stenosis assessment by CT angiography. *JACC Cardiovasc Imaging.* 2013;6:963-72.

14. Kruk M, Noll D, Achenbach S, Mintz GS, Pregowski J, Kaczmarska E, Kryczka K, Pracon R, Dzielinska Z, Sleszycka J, Witkowski A, Demkow M, Ruzyllo W, Kepka C. Impact of coronary artery calcium characteristics on accuracy of CT angiography. *JACC Cardiovasc Imaging.* 2014;7:49-58.

15. Norgaard BL, Gaur S, Leipsic J, Ito H, Miyoshi T, Park SJ, Zvaigzne L, Tzemos N, Jensen JM, Hansson N, Ko B, Bezerra H, Christiansen EH, Kaltoft A, Lassen JF, Botker HE, Achenbach S. Influence of Coronary Calcification on the Diagnostic Performance of CT Angiography Derived FFR in Coronary Artery Disease: A Substudy of the NXT Trial. *JACC Cardiovasc Imaging.* 2015; 8:1045-55.

16. Collet C, Sotomi Y, Cavalcante R, Asano T, Miyazaki Y, Tenekecioglu E, Kistlaar P, Zeng Y, Suwanasson P, de Winter RJ, Nieman K, Serruys PW, Onuma Y. Accuracy of coronary computed tomography angiography for bioresorbable scaffold luminal investigation: a comparison with optical coherence tomography. *Int J Cardiovasc Imaging.* 2017;33:431-9.

17. Doh JH, Koo BK, Nam CW, Kim JH, Min JK, Nakazato R, Silalahi T, Prawira H, Choi H, Lee SY, Namgung J, Kwon SU, Kwak JJ, Lee WR. Diagnostic value of coronary CT angiography in comparison with invasive coronary angiography and intravascular ultrasound in patients with intermediate coronary artery stenosis: results from the prospective multicentre FIGURE-OUT (Functional Imaging criteria for Guiding REview of invasive coronary angiOgraphy, intravascular Ultrasound, and coronary computed Tomographic angiography) study. *Eur Heart J Cardiovasc Imaging.* 2014;15:870-7.

Supplementary data

Supplementary Appendix 1. Study population.
Supplementary Appendix 2. CT acquisition protocol.
Supplementary Appendix 3. CT acquisition parameters.
Supplementary Appendix 4. Objective image quality analysis.
Supplementary Appendix 5. Sample size.
Supplementary Appendix 6. Study endpoints.
Supplementary Appendix 7. Patient flow.
Supplementary Table 1. Comparison of MLA, MLD, and computed FFR values between cCTA and OCT in various kinds of CT scanner.
Supplementary Table 2. Comparison of MLA, MLD, and FFR values between cCTA and OCT in the lesions with low signal-to-noise ratio and intermediate-high signal-to-noise ratio.
Supplementary Table 3. Comparison of MLA, MLD, and FFR values between cCTA and OCT in the lesions with low contrast-to-noise ratio and intermediate-high contrast-to-noise ratio.
Supplementary Table 4. Comparison of MLA, MLD, and FFR values between cCTA and OCT in the lesions with image quality scale 2, 3 and image quality scale 4, 5.
Supplementary Table 5. Passing and Bablok regression analysis.
Supplementary Table 6. Comparison of MLA, MLD, and FFR values between cCTA and OCT in the lesions with a combination of MLD ≥1.0 mm/low-intermediate and high AS.
Supplementary Table 7. Comparison of MLA, MLD, and FFR values between cCTA and OCT in the lesions with a combination of MLD <1.0 mm/low-intermediate and high AS.
Supplementary Figure 1. The size of OCT catheter and guidewire.
Supplementary Figure 2. Impact of image quality on the relation between cCTA MLA and OCT MLA.
Supplementary Figure 3. Distribution of AS.
Supplementary Figure 4. Concordance rate for diagnosis of ischaemia between FFR_{CT} and FFR_{OCT}.
Supplementary Figure 5. A case with discordant diagnosis between FFR_{CT} and FFR_{OCT}.
Supplementary Figure 6. Cases with concordance between FFR_{CT} and FFR_{OCT}.
Supplementary Figure 7. Cases with discordance between FFR_{CT} and FFR_{OCT}.
Supplementary Figure 8. cCTA vs. OCT measurement.

The supplementary data are published online at:
http://www.pcronline.com/
eurointervention/148th_issue/274

Supplementary data

Supplementary Appendix 1. Study population

At 2 centres in Japan (Kobe University Hospital and Akashi Medical Center), 100 patients with available preprocedural cCTA and OCT data were enrolled. Patients >20 years old who underwent clinically indicated invasive coronary angiography and OCT with preprocedural cCTA were eligible for inclusion. Among such patients, lesions with a percentage diameter stenosis between 25% and 75% by angiography were considered for quantitative cCTA and OCT analysis. Patient-based exclusion criteria included non-cardiac illness with life expectancy <2 years; pregnancy; allergy to iodinated contrast; estimated glomerular filtration rate <30 mL/min/1.73 m^2; significant arrhythmia; heart rate ≥100 beats/min; systolic blood pressure <90 mmHg; contraindication to beta-blockers or nitroglycerine; prior coronary artery bypass surgery; or poor cCTA/OCT image quality. Lesion-based exclusion criteria included ruptured plaque, ectasia, small vessels (reference lumen diameter <2.0 mm), and stented vessels.

Supplementary Appendix 2. Study endpoints

The pre-specified primary endpoint of the study was the correlation between cCTA and OCT for MLA measurements. Secondary endpoints included the correlation between FFR_{CT} and FFR_{OCT}, and the effect of calcification on the agreement between MLA and FFR values derived from CT and OCT.

Supplementary Appendix 3. CT acquisition protocol

cCTA images were obtained in accordance with the Society of Cardiovascular Computed Tomography (SCCT) guidelines on cCTA. Oral beta-blockers were administered in subjects with heart rates ≥65 beats/min. Immediately before cCTA acquisition, 0.3 mg sublingual nitroglycerine was administered to all patients.

Supplementary Appendix 4. CT acquisition parameters

All examinations were performed with Aquilion one (320×0.5 mm section collimation), Aquilion 64 (64×0.6 mm section collimation; Toshiba, Otawara, Japan), Somatom Definition Flash (128×0.6 mm section collimation; Siemens, Forchheim, Germany), and Ingenuity Core (128×0.5 mm section collimation; Philips, Surrey, United Kingdom). The scan parameters included 100–120 kVp tube voltage, and 260–1,150 mA tube current (depending on body habitus). All images were reconstructed using thin slices (0.5–0.75 mm) and medium smooth reconstruction filters in different phases.

Supplementary Appendix 5. Objective image quality analysis

For objective image analysis, dedicated post-processing and evaluation software (Ziostation 2, Ziosoft) was used. Attenuation measurements were obtained by the same observer by drawing ROIs in the proximal reference of the lesion, scaled as large as possible whilst carefully avoiding vessel walls or plaques. Image noise was defined as the standard deviation of CT measurements in an ROI in the aortic root. To determine vessel contrast, the CT attenuation of the chest subcutaneous fat tissue, adjacent to the vessel contour, was measured. Signal-to-noise ratios (SNRs) and contrast-to-noise ratios (CNRs) were calculated for each measurement, as follows:

$SNR = Attenuation_{lesion}/Noise$

$CNR = Attenuation_{lesion - fat}/Noise$

Image quality of the lesion was assessed on a 5-point Likert scale: 5 = excellent with no
granularity, no or minimal artefacts and clear vessel display; 4 = between 5 and 3; 3 =
acceptable for diagnosis, but small amounts of radiation and high density or irregular
low density artefacts and fuzzy boundaries were present; 2 = suboptimal with some
artefacts, but acceptable; and 1 = diagnostic decision cannot be made due to blurry
boundaries and large amounts of radiation, high density or irregular low density
artefacts as previously reported.

Supplementary Appendix 6. Sample size

The sample size of 71 lesions was determined on the basis of a previously reported
correlation of 0.53 between intravascular ultrasound and cCTA, assuming that the
correlation coefficient of the lumen area of cCTA and OCT was at least r=0.4 or higher,
and a 95% power with a 2-sided alternative hypothesis and a type I error of 5% [17].

Supplementary Appendix 7. Patient flow

From 100 patients, 137 vessels were considered for inclusion in the present study.
Sixty-five vessels were excluded due to ruptured plaque or ectasia (n=6), poor cCTA
image quality (n=17), poor OCT image quality (motion/misregistration, high image
noise, or low contrast to noise) (n=9), reference diameter <2.0 mm (n=16), or stents
(n=17). Finally, 72 vessels (118 lesions) in 57 patients were included for MLA
evaluation by cCTA and OCT. Eight vessels were excluded from FFR computation by
cCTA and OCT due to the lack of side branches, which precluded the merging process

that required at least 2 branches to match lesion locations precisely. Accordingly, we assessed the difference between cCTA and OCT-based FFR in 64 vessels representing 52 patients **(Figure 2)**.

Supplementary Table 1. Comparison of MLA, MLD, and computed FFR values between cCTA and OCT in various kinds of CT scanner.

	64-slice CT (n=53)			128-slice CT (n=61)			320-slice CT (n=4)		
	cCTA	OCT	*p*-value	cCTA	OCT	*p*-value	cCTA	OCT	*p*-value
MLA (mm^2)	2.08±1.40	2.13±1.48	0.889	2.01±1.31	2.04±1.24	0.924	3.10±0.96	3.09±1.50	0.997
MLD (mm)	0.77±0.26	0.78±0.27	0.913	0.76±0.26	0.77±0.24	0.793	0.99±0.16	0.98±0.24	0.966
Computed FFR	0.74±0.15	0.78±0.11	0.287	0.74±0.16	0.80±0.12	0.110	0.81±0.03	0.84±0.05	0.612
Absolute MLA error	0.71±0.54		NA	0.57±0.52		NA	0.38±0.08		0.442[#] 0.237[##]
Absolute FFR error	0.07±0.10		NA	0.06±0.07		NA	0.06±0.08		0.760[#] 0.676[##]

Values are median ± SD. Abbreviations as in Tables 1 and 2. # *p*-value for 64-slice vs. 128-slice vs. 320-slice CT.

p-value for 64-slice vs. others.

Supplementary Table 2. Comparison of MLA, MLD, and FFR values between cCTA and OCT in the lesions with low signal-to-noise ratio and intermediate-high signal-to-noise ratio.

	Low signal-to-noise ratio (39 lesions, 24 vessels)			Intermediate-high signal-to-noise ratio (79 lesions, 48 vessels)		
	cCTA	OCT	*p*-value	cCTA	OCT	*p*-value
MLA (mm^2)	2.29±1.33	2.49±1.30	0.610	1.97±1.31	1.93±1.32	0.878
MLD (mm)	0.81±0.26	0.86±0.24	0.555	0.75±0.25	0.75±0.24	0.923
FFR value	0.794±0.112	0.821±0.114	0.462	0.720±0.159	0.765±0.109	0.92

Values are median ± SD. Abbreviations as in Tables 1 and 2.

Supplementary Table 3. Comparison of MLA, MLD, and FFR values between cCTA and OCT in the lesions with low contrast-to-noise ratio and intermediate-high contrast-to-noise ratio.

	Low contrast-to-noise ratio (39 lesions, 24 vessels)			Intermediate-high contrast-to-noise ratio (79 lesions, 48 vessels)		
	cCTA	OCT	*p*-value	cCTA	OCT	*p*-value
MLA (mm^2)	1.93±1.30	1.81±1.06	0.759	2.14±1.33	2.24±1.43	0.707
MLD (mm)	0.74±0.25	0.73±0.21	0.891	0.78±0.26	0.80±0.26	0.696
FFR value	0.800±0.124	0.837±0.087	0.295	0.718±0.154	0.769±0.116	0.086

Values are median ± SD. Abbreviations as in Tables 1 and 2.

Supplementary Table 4. Comparison of MLA, MLD, and FFR values between cCTA and OCT in the lesions with image quality scale 2, 3 and image quality scale 4, 5.

	Image quality scale 2, 3 (28 lesions, 18 vessels)			Image quality scale 4, 5 (90 lesions, 54 vessels)		
	cCTA	OCT	*p*-value	cCTA	OCT	*p*-value
MLA (mm^2)	2.01±1.43	2.00±1.43	0.976	2.48±1.61	2.51±1.51	0.903
MLD (mm)	0.76±0.26	0.76±0.26	0.987	0.84±0.28	0.86±0.26	0.746
FFR value	0.719±0.131	0.768±0.112	0.300	0.751±0.154	0.797±0.112	0.100

Values are median ± SD. Abbreviations as in Tables 1 and 2.

Supplementary Table 5. Passing and Bablok regression analysis.

	cCTA MLA vs. OCT MLA		FFR$_{CT}$ vs. FFR$_{OCT}$	
	Intercept (95% CI)	Slope (95% CI)	Intercept (95% CI)	Slope (95% CI)
All lesions (n=118)	0.084 (-0.116 to 0.330)	0.970 (0.870 to 1.095)	0.119 (-0.020 to 0.234)	0.889 (0.750 to 1.000)
Low-intermediate AS (n=79)	0.145 (-0.092 to 0.396)	0.959 (0.859 to 1.074)	0.129 (-0.013 to 0.282)	0.882 (0.692 to 1.059)
High AS (n=39)	0.036 (-0.606 to 0.448)	0.948 (0.708 to 1.442)	0.138 (-0.048 to 0.286)	0.863 (0.680 to 1.083)
MLD ≥1.0 mm (n=93)	0.154 (-0.162 to 0.432)	0.970 (0.851 to 1.122)	0.122 (0.020 to 0.222)	0.886 (0.769 to 1.000)
MLD <1.0 mm (n=25)	0.733 (0.628 to 0.788)	0.086 (0.003 to 0.199)	0.295 (-0.098 to 0.513)	0.657 (0.333 to 1.167)

95% CI: 95% confidence interval. Other abbreviations as in Table 1.

Supplementary Table 6. Comparison of MLA, MLD, and FFR values between cCTA and OCT in the lesions with a combination of MLD ≥1.0 mm/low-intermediate and high AS.

	MLD ≥1.0 mm (93 lesions, 60 vessels)			MLD ≥1.0 mm/low-intermediate AS (62 lesions, 38 vessels)			MLD ≥1.0 mm/high AS (31 lesions, 21 vessels)		
	cCTA	OCT	*p*-value	cCTA	OCT	*p*-value	cCTA	OCT	*p*-value
MLA (mm^2)	2.72±1.57	2.80±1.45	0.732	2.87±1.62	2.98±1.50	0.697	2.43±1.44	2.44±1.27	0.981
MLD (mm)	1.79±0.50	1.83±0.46	0.606	1.84±0.51	1.89±0.47	0.592	1.70±0.47	1.71±0.43	0.899
FFR value	0.792±0.108	0.823±0.098	0.166	0.791±0.106	0.828±0.097	0.211	0.794±0.113	0.813±0.101	0.546

Values are median ± SD. Abbreviations as in Tables 1–3.

Supplementary Table 7. Comparison of MLA, MLD, and FFR values between cCTA and OCT in the lesions with a combination of MLD <1.0 mm/low-intermediate and high AS.

	MLD <1.0 mm (25 lesions, 23 vessels)			MLD <1.0 mm/low-intermediate AS (17 lesions, 14 vessels)			MLD <1.0 mm/high AS (8 lesions, 7 vessels)		
	cCTA	OCT	*p*-value	cCTA	OCT	*p*-value	cCTA	OCT	*p*-value
MLA (mm²)	1.05±0.79	0.86±0.14.	0.238	1.06±0.89	0.88±0.15	0.421	1.04±0.57	0.82±0.13	0.317
MLD (mm)	1.09±0.41	1.04±0.09	0.608	1.07±0.45	1.05±0.88	0.863	1.11±0.32	1.02±0.08	0.439
FFR value	0.644±0.179	0.722±0.116	0.101	0.625±0.197	0.731±0.126	0.105	0.681±0.144	0.706±0.985	0.719

Values are median ± SD. Abbreviations as in Tables 1–3.

Supplementary Figure 1. The size of OCT catheter and guidewire.
A) Size chart of the devices, B) schematic illustration of OCT catheter and guidewire with lumen, C) size of circumscribed ellipse (i.e., simulated lumen) that contains OCT catheter and guidewire.

B)

0.9 mm
Catheter

0.356 mm
Guide wire
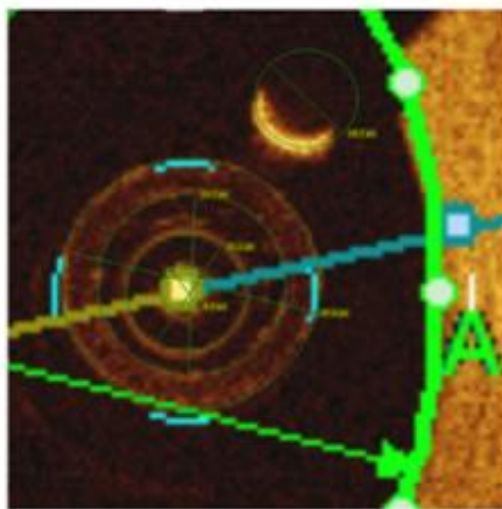
A)

	inch	mm	pixel
Guide wire	0.0140	0.356	18.7
Catheter-outer	0.0354	0.900	47.4
Catheter-inner	0.0252	0.639	33.7
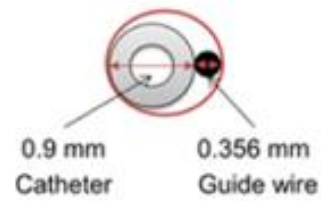
C)
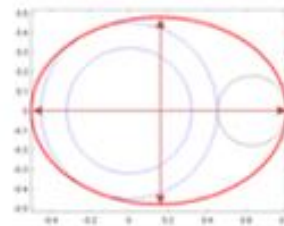
Bounding ellipse size
Diameter: Long Axis = 1.308 mm
: Short Axis = 0.957 mm

Supplementary Figure 2. Impact of image quality on the relation between cCTA MLA and OCT MLA.

A) Impact of signal-to-noise ratio.

a) Low signal-to-noise ratio, b) intermediate-high signal-to-noise ratio.

B) Impact of contrast-to-noise ratio.

a) Low contrast-to-noise ratio, b) intermediate-high contrast-to-noise ratio.

C) Impact of five-point Likert scale.

a) Likert scale 2, 3, b) Likert scale 4, 5.

Supplementary Figure 2 (A) Impact of signal-to-noise ratio
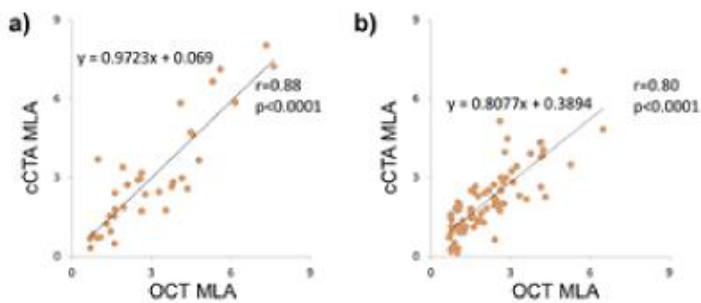
Supplementary Figure 2 (B) Impact of contrast-to-noise ratio
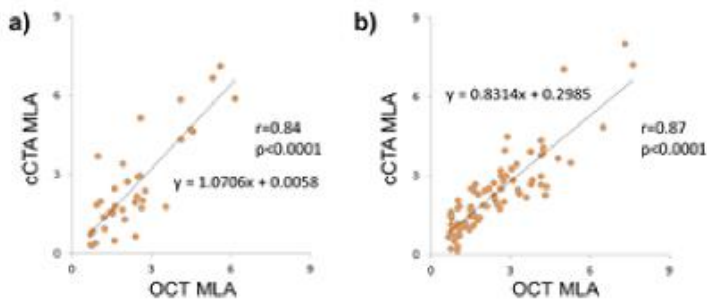
Supplementary Figure 2 (C) Impact of five-point Likert scale
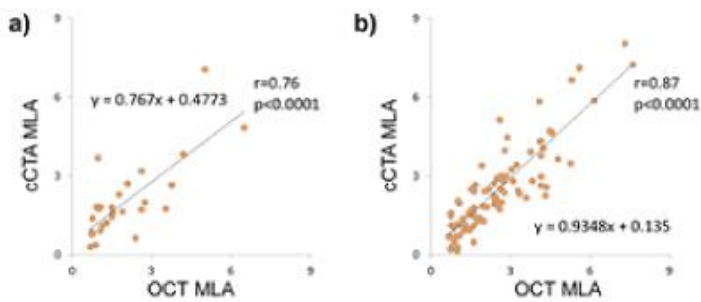
Supplementary Figure 3. Distribution of AS.

A) Per-lesion distribution of AS, B) per-vessel distribution of AS.
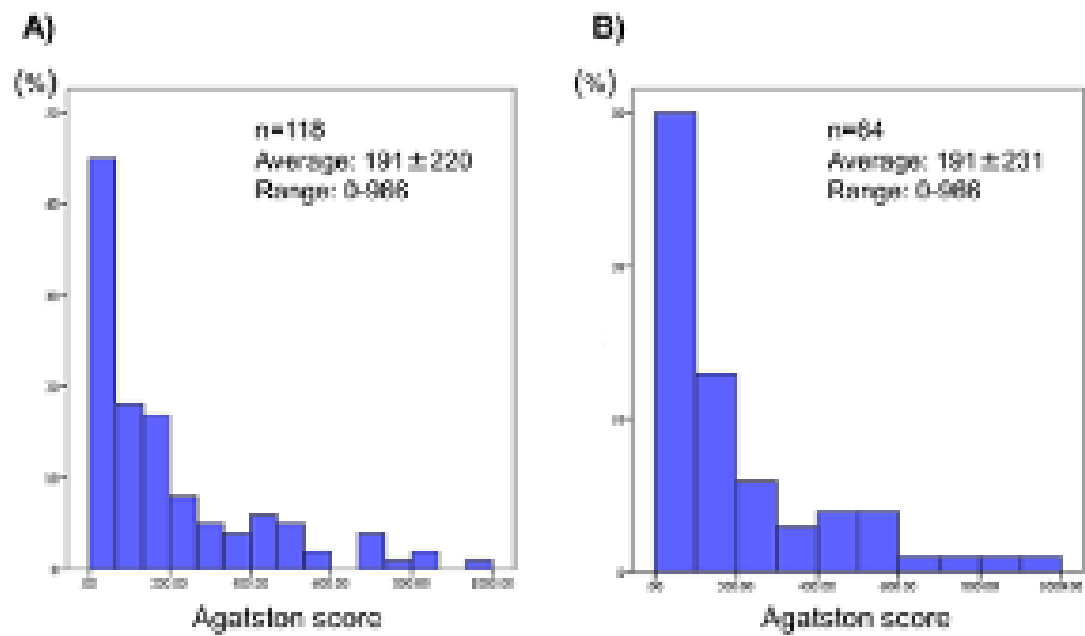
Supplementary Figure 4. Concordance rate for diagnosis of ischaemia between FFR_{CT} and FFR_{OCT}.
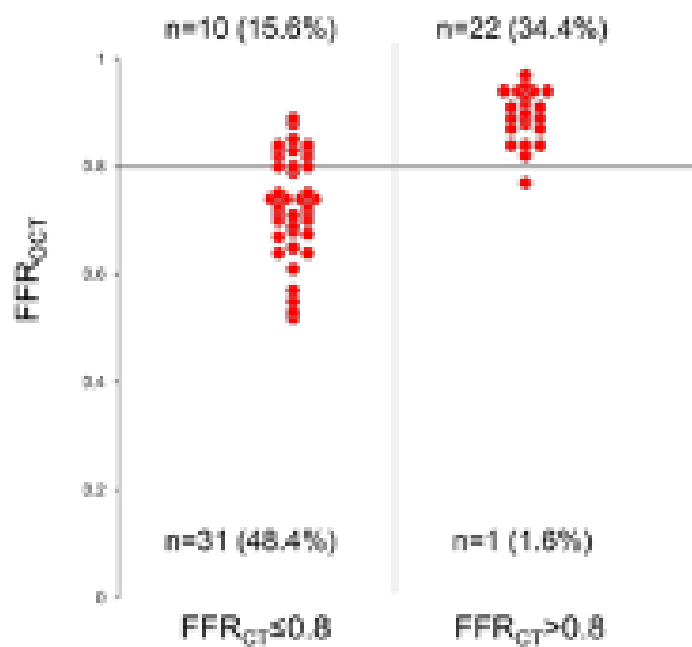
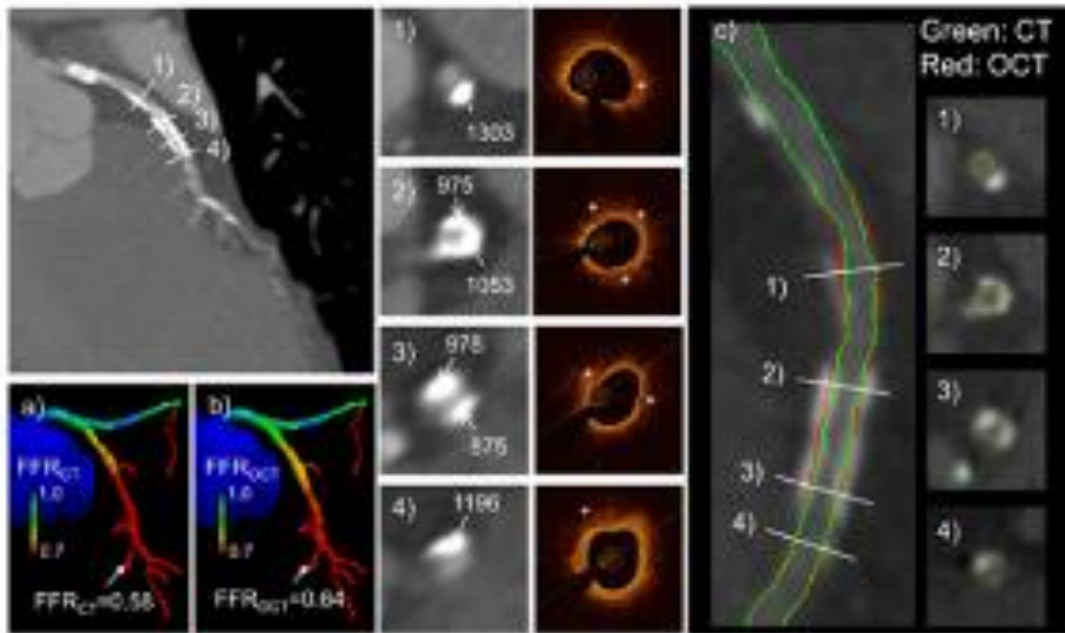**Supplementary Figure 5.** A case with discordant diagnosis between FFR$_{CT}$ and FFR$_{OCT}$.

a) With wire insertion; b) without wire insertion; c) FFR$_{CT}$; d) FFR$_{OCT}$; e) co-registered cCTA/OCT image. 1, 2): Cross-sectional images from cCTA and OCT. There was a focal stenosis in the position 1) with wire insertion (a); however, there was no stenosis without wire insertion in the same position (b). Cross-sectional OCT image of 1) showed smaller lumen diameter than that of 2). These images suggest the accordion phenomenon induced by wire insertion in this case.
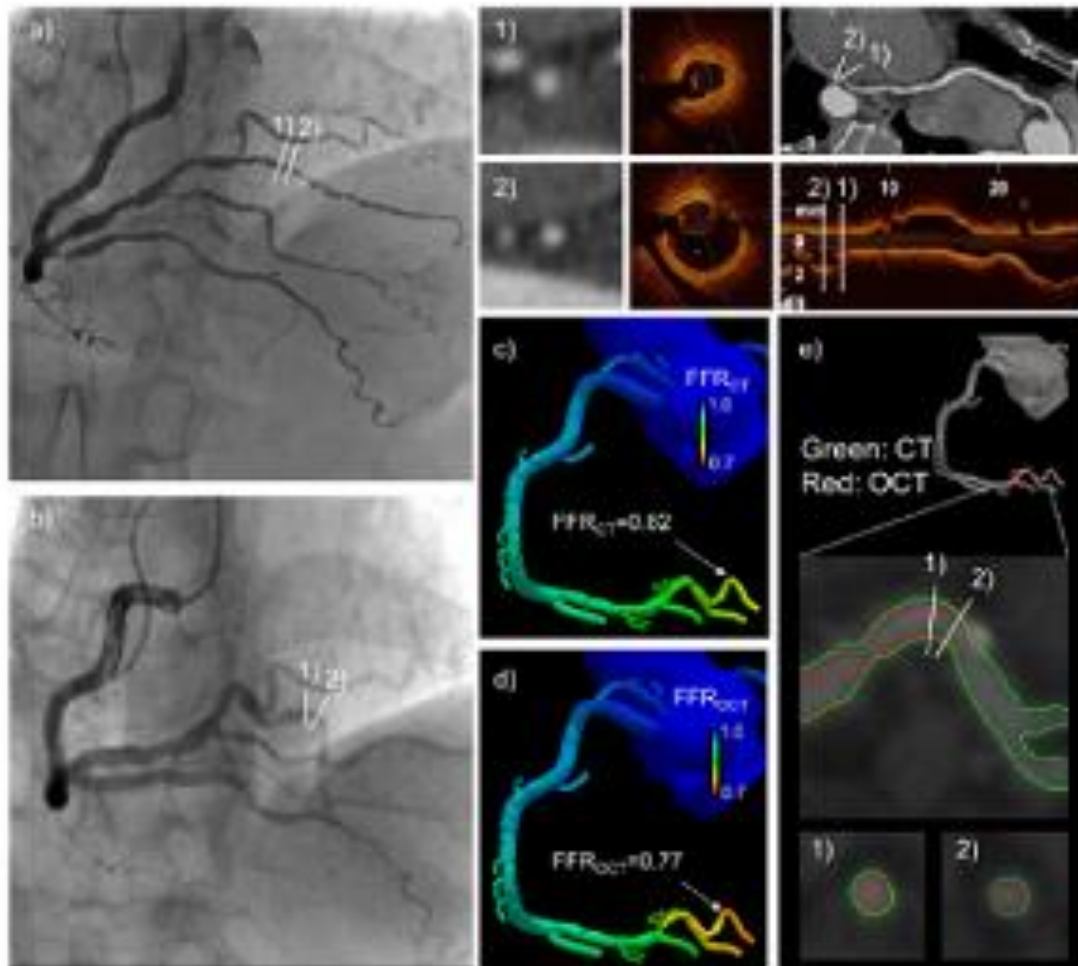
Supplementary Figure 6. Cases with concordance between FFR$_{CT}$ and FFR$_{OCT}$. The case with severe calcification (per-vessel AS: 549); FFR$_{CT}$: 0.58, FFR$_{OCT}$: 0.64, 1)-4) cross-sectional images from cCTA and OCT; asterisk indicates calcification. a) FFR$_{CT}$, b) FFR$_{OCT}$, and c) co-registered cCTA/OCT image.
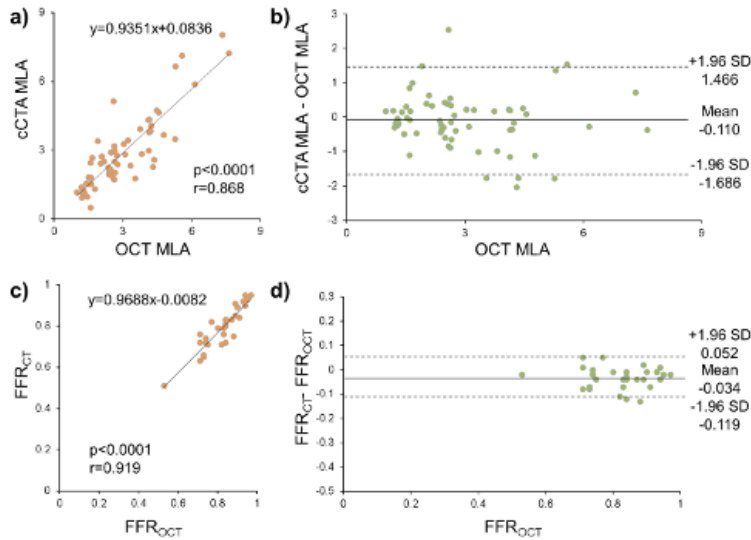
Supplementary Figure 7. Cases with discordance between FFR$_{CT}$ and FFR$_{OCT}$. The case with focal calcification (per-vessel AS: 31); FFR$_{CT}$: 0.71, FFR$_{OCT}$: 0.82, 1)-4) cross-sectional images from cCTA and OCT; asterisk indicates calcification. a) FFR$_{CT}$, b) FFR$_{OCT}$, and c) co-registered cCTA/OCT image.
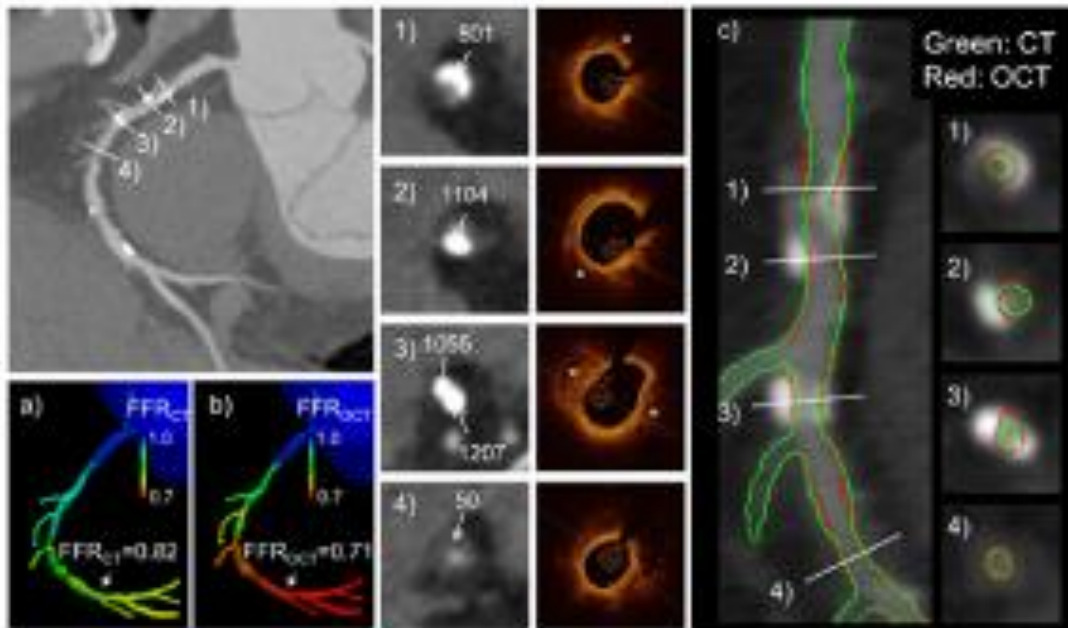
Supplementary Figure 8. cCTA vs. OCT measurement.
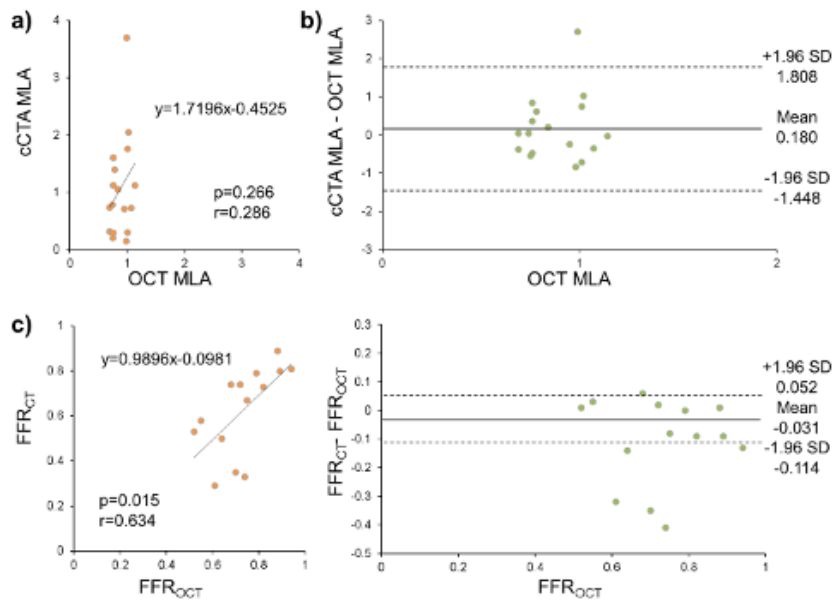
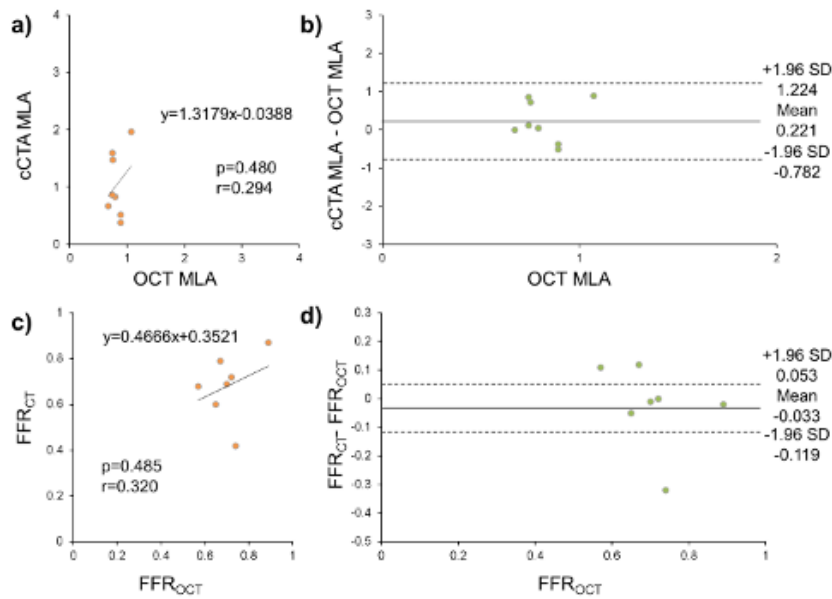**Supplementary Figure 8 A)**

Supplementary Figure 8 B)
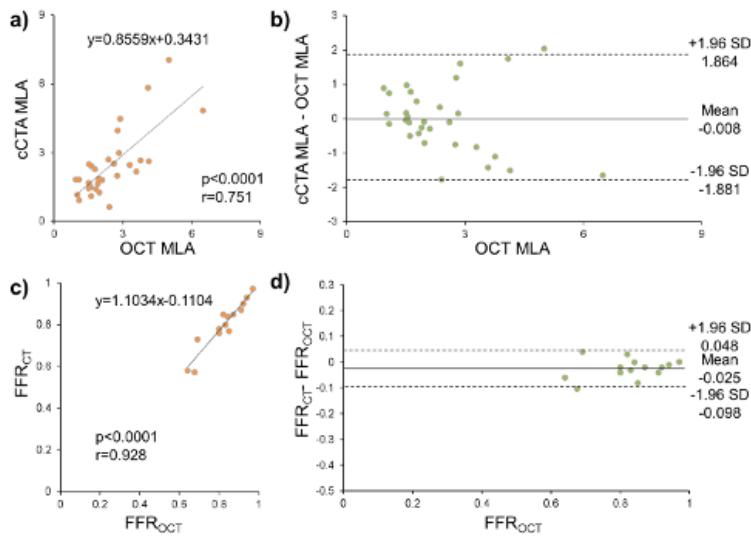
A) Lesions with MLD ≥1.0 mm and a low-intermediate AS, B) lesions with MLD ≥1.0 mm and a severe AS. a) Correlation between MLA from cCTA and OCT; b) Bland-Altman plots of cCTA MLA vs. OCT MLA; c) correlation between FFR from cCTA and OCT; d) Bland-Altman plots of FFR_{CT} versus FFR_{OCT}.

Supplementary Figure 8 C)

Supplementary Figure 8 D)

C) Lesions with MLD <1.0 mm and a low-intermediate AS, D) lesions with MLD <1.0 mm and a severe AS. a) Correlation between MLA from cCTA and OCT; b) Bland-Altman plots of cCTA MLA vs. OCT MLA; c) correlation between FFR from cCTA and OCT; d) Bland-Altman plots of FFR_{CT} versus FFR_{OCT}.